SCIENCE CHINA
Technological Sciences

•Article•

December 2018 Vol.61 No.12: 1814–1823
https://doi.org/10.1007/s11431-017-9237-6

Experimental research on the heating performance of a single cylinder refrigerant injection rotary compressor heat pump with flash tank

SUN JinFei[1,2,3,4], ZHU DongSheng[1,2,3*], YIN YingDe[1,2,3] & LI XiuZhen[1,2,3,4]

[1] *Guangzhou Institute of Energy Conversion, Chinese Academy of Sciences, Guangzhou 510640, China;*
[2] *Key Laboratory of Renewable Energy, Chinese Academy of Sciences, Guangzhou 510640, China;*
[3] *Guangdong Key Laboratory of New and Renewable Energy Research and Development, Guangzhou 510640, China;*
[4] *University of Chinese Academy of Sciences, Beijing 100049, China*

Received September 10, 2017; accepted March 19, 2018; published online May 11, 2018

A single cylinder rotary compressor was applied in the refrigerant injection air-source heat pump to improve the heating performance in cold regions. In this study, the performance of an R410A single cylinder rotary compressor vapor injection (SCRCVI) system was measured and analyzed by varying the compressor frequency f and injection pressure P_{inj} at the ambient temperature T_{od}=–10°C.The experimental results indicated that an optimum injection pressure to gain the maximum COP_h (coefficient of performance) existed in the SCRCVI cycle. However, the maximum COP_h of the SCRCVI system decreased as the increase of the frequency, and the maximum COP_h was even lower than that of the CSVC system at high compressor frequency. Therefore, in view of the energy saving and emission reduction, the SCRCVI system should be switched to single stage compression system when the heating capacity demand could be satisfied at high compressor frequency f. Compared to the conventional single-stage vapor compression (CSVC) system, refrigerant injection could enhance the heating capacities and COP_h by 28.2% and 7.91%, respectively. The average total mass flow rate of the SCRCVI system was 24.68% higher than that of the CSVC system. As the SCRCVI system worked at the optimum injection pressure, the variation trends of the different system parameters were investigated in detail. These trends were reliably used to optimize the refrigerant injection system design and the control strategy. The parameter of (P_{inj}–P_s) could be adopted as the signals to control the opening of the upper stage electronic expansion valve EEV1.

rotary compressor, refrigerant injection, DC (direct current) inverter, heat pump, heating performance, injection pressure

Citation: Sun J F, Zhu D S, Yin Y D, et al. Experimental research on the heating performance of a single cylinder refrigerant injection rotary compressor heat pump with flash tank. Sci China Tech Sci, 2018, 61: 1814–1823, https://doi.org/10.1007/s11431-017-9237-6

1 Introduction

With the economic development and population increase, the contradiction between increasing energy demand and energy shortage is intensifying. Therefore, the energy saving has become the crucial problems. Although the air-source heat pump is one of the most convenient and economical ways to utilize the low-grade energy, the conventional single-stage vapor compression (CSVC) system cannot be widely applied in cold regions due to the dramatic performance degradation. In order to overcome the above problem, researchers have proposed some sorts of solutions to enhance the heating performance, such as refrigerant injection [1–3], additional heat source [4], cascade system [5,6], the application of

* Corresponding author (email: zhuds@ms.giec.ac.cn)

electronic expansion valve [7], dual source/ground source heat pump [8,9], and inverter technology [10]. In the past decades, applications of refrigerant injection and inverter technology to the air-source heat pump have received more attentions since it could improve system performance effectively and ensure the compressor works reliably.

The flash tank vapor injection (FTVIC) system has been applied to air conditioners since 1979 [2,11]. Moreover, the FTVIC system could adjust the capacity by changing the intermediate pressure, compressor frequency, and the injection ratio. After a review of previous literatures, we conclude that the thermodynamic analysis and experimental research are the main approaches to investigate the system performance of FTVIC system.

For the thermodynamic study, Qiao et al. [11] analyzed the dynamic behavior of an R410A FTVIC system with scroll compressor by developing a transient, lumped-parameter model, and concluded that the major transient flow characteristics and heat transfer can be captured by the proposed model, which was successfully verified by the experimental data of reference [12]. As a continuation and extension of previous work, Qiao et al. [13] developed a detailed frost growth model of a heat exchanger to explore the frosting dynamics of a two-stage flash tank vapor injection heat pump system, and found that air and refrigerant flow maldistribution, resulting from non-uniform frost growth on the outdoor heat exchanger, could lead to unstable system hunting behavior. Redón et al. [14] gave attention to optimizing the system performance and set up the several thermodynamic vapor injection models working with different refrigerants (R32, R290, R407C, and R22), and found that the COP_h of FTVIC system could be improved by 30% over the non-injection systems, and a bad system design could cause a loss of improvement between 6% and 10%. Wang et al. [15] thermodynamically modeled an FTVIC system with a newly designed hybrid economizer and concluded that the hybrid economizer could enhance the cooling capacity by 1.5%–3.5% and provided the condition for the application of thermostatic expansion valve (TXV) by generating the superheated vapor. The same author also has given attention to the dynamic work process of the scroll compressor [16–18] and proposed that the injection process could be considered as a continuous "adiabatic throttling+isobaric mixing" process. Park et al. [19] evaluated an FTVIC system with a scroll compressor and concluded that the geometrical parameters of the injection port and thermodynamic injection parameters had a significant effect on the compressor characteristics. Cho et al. [20] investigated the characteristic distinction between the symmetric and asymmetric compressor by a simplified thermodynamic model under different working conditions, and found that increasing injection porthole area could overcome performance degradation when the frequency increased. Dardenne et al. [21] built a semi-empirical model to evaluate the compressor macroscopic performance of the scroll compressor. The comparisons between the predicted and the experimental data indicated that 89%–98% of predicted data showed good accuracy.

For the experimental work, Heo et al. [22] built a test-bed to explore the variation of the heating performance and concluded that the improvement of heating capacity was more obvious at high compressor frequencies and low ambient temperatures for the FTVIC system. Compared with the non-injection system, the total mass flow rate of FTVIC system improved by 30%–38%. Wang et al. [23] tested an R410A FTVIC system, and found that the improvements of the FTVIC system capacity and COP_h were about 14% and 4%, 30% and 20%, respectively, relative to those of the non-injection system, which has the same displacement volume, at the ambient temperature of 46.1°C and –17.8°C. The heating performances of the FTVIC system and the subcooler vapor injection (SCVIC) system were compared experimentally by Ma and Zhao [24] using R22 as working fluid. The refrigerant injection with flash tank could improve the heating capacity and COP_h by 10.5% and 4.3%, respectively, compared with those of the SCVIC system. Xu et al. [25] tested the FTVIC system in the transient and steady-state process, and found that the electronic expansion valve coupled with the PID controller is an effective way to adjust the injection ratio and 4–6 K degree superheat for the injected vapor is appropriate with the purpose of high performance and feasibility. Then Xu et al. [26] conducted a series of experiments to compare the performance difference between R410A and R32 in the identical FTVIC system. Baek et al. [27,28] experientially tested the FTVIC system with the working fluid of CO_2. The test result showed that under the optimum injection ratio, the Q_h and maximum COP_h of the FTVIC system were 10.7% and 6.7% higher than those of the CSVC system under the same testing conditions.

Previous researches almost focused on the vapor injection techniques applied to scroll compressor or twin rotary compressor. However, the scroll compressor was designed with a fixed volume ratio. As the working condition changed, the over-compression and under-compression are prone to occur for the scroll compressor. While for the conventional twin rotary compressor, it has two separate cylinders and a mixing chamber. The compressions and injection processes of conventional twin rotary compressor are independent due to the existence of the intermediate mixture chamber. Compared with the single cylinder rotary compressor, the twin rotary compressor is more expensive and has more easily-worn parts, which are not conductive to improve the cost-effective for the minitype residential air conditioners. Therefore, in order to further reduce the cost of the compressor for low ambient temperature heating, applying the refrigerant injection technology in single cylinder rotary compressor attracts the interest of researchers recently. The

cylinder injection and blade injection are the two main types of vapor injection technology used in single cylinder rotary compressor. For the cylinder injection, Jia et al. [29] investigated the heating performance of an R410A FTVIC system by experiments under different ambient temperatures. The injection pressure was fixed at the optimum value for different systems. The test results indicated that the heating capacity Q_h and COP_h were improved by 2.29% and 1.94%, respectively, compared with those of the twin cylinder vapor-injected rotary compressor system when the ambient temperature was above −15°C. Their further research found that the improvement of the single cylinder vapor-injected rotary compressor system heating capacity was more than 12% as well as APF (annual performance factor) increased by 4.62%, compared with those of the CSVC system when the ambient temperature was higher than −15°C [30]. For the blade injection, Wang et al. [31–33] investigated the performance of the air source heat pump by simulation based on a verified numerical model. The results under different ambient temperatures showed that the blade injection could overcome the back-flow of the cylinder injection and enhance heating capacity and COP_h of the air source heat pump by 23.1%–28.2% and 4.5%–8.1%, respectively, compared with the CSVC system with a regular single-stage rotary compressor.

The studies above indicated the single cylinder rotary compressor with different injection structure could enhance the heating performance significantly like the vapor-injected scroll compressor/twin cylinder rotary compressor under low ambient temperature. The existing researches mainly focused on the variation of heating performance with ambient temperature. There are few researches on the variation of heating performance with injection pressure and compressor frequency for a single cylinder vapor-injected rotary compressor at present.

To evaluate the effects of injection pressure and compressor frequency on the system performance, an R410A FTVIC system with single cylinder vapor-injected rotary compressor was built in this study. The heating performance of the R410A SCRCVI system and the CSVC system were measured and analyzed for comparison. The experimental results will be evaluated for use in the future optimization of the injection structure and the control strategy.

2 Single cylinder rotary compressor

The injection hole and reed valve were installed on the cylinder of rotary compressor (as shown in Figure 1). The working processes of the rotary compressor are stated as Figure 2(a)–(d). It includes four processes in each rotation period: the suction, the refrigerant injection, the compression, and the discharge. The refrigerant is injected into the working chamber as the meshing line of the piston rotating over the suction port. When the pressure of working chamber is larger than the injection pressure, the reed valve, settled on the injection hole, will be closed with the proposed of stopping the vapor reflux. Then the refrigerant vapor would be further compressed and the working chamber pressure will reach to the discharge pressure. The compression & discharge process is starting. The injection pressure could theoretically change from the evaporation pressure to the condensing pressure. For the rotary compressor, the variation of the working chamber pressure is shown in Table 1. It should be noted that as the rotor rotates from the injection hole to the suction port, the injected gas will flow into the suction tube, which will decrease the volume efficiency of the compressor at the suction process.

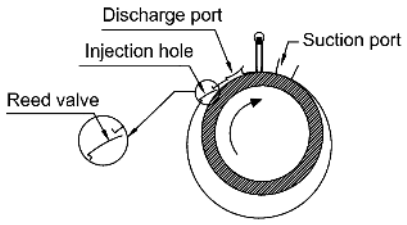

Figure 1 Structure of rotary compressor.

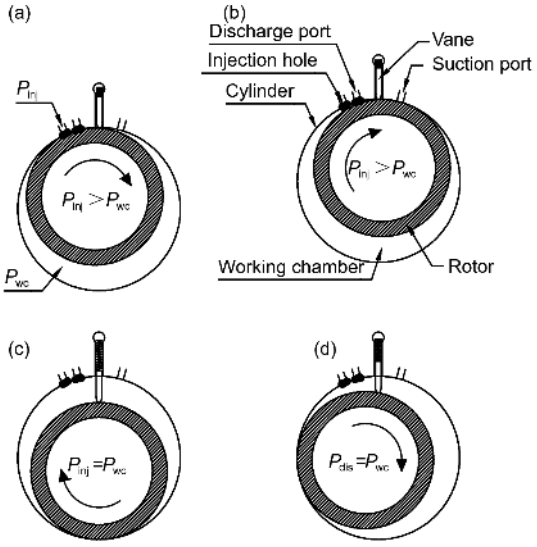

Figure 2 Schematic diagram of working process in cylinder. (a) Suction; (b) injection & compression; (c) compression; (d) discharge.

3 Experimental setup and test procedure

3.1 Experimental setup

A test-bed of an air-source heat pump with the flash tank was built. The refrigerant injection technique coupled with the inverter rotary compressor was applied in the system under the testing condition. Figure 3 illustrated the schematic dia-

Table 1 Variation of the working chamber pressure

Processes	Specifications
Suction	$P_{inj} > P_{wc}$
Refrigerant injection	$P_{inj} > P_{wc}$
Compression	$P_{inj} \leq P_{wc}$
Discharge	$P_{wc} = P_{dis}$

gram of the R410A SCRCVI test-bed. The thermo-mechanical analysis is shown in Figure 4. The experimental setup was initially equipped with a 4-way reversing valve, a single cylinder rotary compressor, a flash tank, a ball valve, an upper-stage electronic expansion valve (EEV1), the indoor & outdoor heat exchanger, and a lower-stage electronic expansion valve (EEV2). The indoor heat exchanger and outdoor heat exchanger were mounted separately in two closed environment chambers. The single cylinder rotary compressor was driven by a DC inverter. The upper-stage EEV1 was equipped at the inlet of the flash tank to control the injection pressure and the injection mass flow rate. The function of lower-stage EEV2 was to control the superheated degree of the suction vapor in the range of 3–5 K. The working condition of the system could be changed by shutting off the ball valve installed on the injection pipe. It meant that the SCRCVI system was turned into the CSVC system when the ball valve was shut off. As the compressor frequency was fixed at a certain value, the injection pressure could be changed by adjusting the opening of the EEV1. In the meantime, the EEV2 was automatically adjusted depending on the superheated degree of the suction vapor. The specifications of the main components are illustrated in Table 2.

3.2 Test condition

In the present study, only the heating model without frosting condition was considered. The experiment condition was shown in Table 3. This setup used R410A as the working fluid. The heating performance of the SCRCVI system was comprehensively investigated under different compressor frequency f and different injection pressure P_{inj}. The comparison heating performance test of CSVC system was conducted under different compressor frequency at the same experiment condition. Moreover, when the injection pressure was lower, the injected refrigerant was vapor. When the injection pressure increased to high enough, two-phase refrigerant was injected into the rotary compressor from the injection pipe.

3.3 Data analysis method

The system heating COP_h, air-side capacity, refrigerant-side capacity and refrigerant-side mass flow rate are calculated from eqs. (1)–(6). The power consuming W was acquired by a power meter. The deviations between the measured value and theoretical derivation value at the base of energy balance were within 4%.

Air-side mass flow rate

$$\dot{m}_{air} = K \times \sqrt{\frac{\Delta P}{\rho}}. \tag{1}$$

Heating capacity

$$Q_h = \dot{m}_{air} \times (h_{out} - h_{in}). \tag{2}$$

Coefficient of performance

$$COP_h = \frac{Q_h}{W}. \tag{3}$$

Injection mass flow rate

$$\dot{m}_{inj} = \dot{m}_{to} - \dot{m}_{eva}. \tag{4}$$

The injection mass flow ratio

$$R_m = \frac{\dot{m}_{inj}}{\dot{m}_{to}}. \tag{5}$$

The injection pressure ratio

$$R_p = \frac{P_{inj} - P_s}{P_{dis} - P_s}. \tag{6}$$

The calibration of all the measuring instruments was

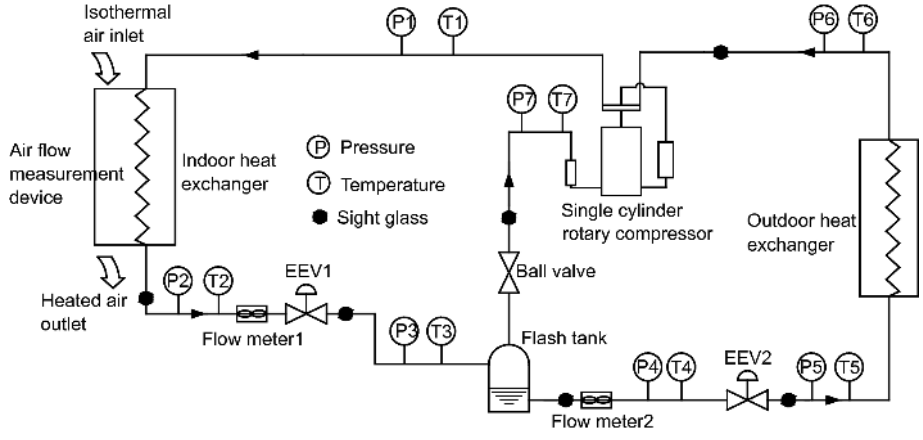

Figure 3 Schematic diagram of the experimental setup.

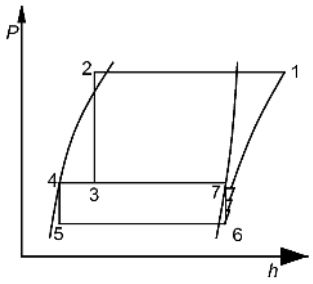

Figure 4 Pressure-enthalpy diagram.

conducted before testing. The measurement uncertainties for the key parameters were shown in Table 4. The theory of propagation of errors including systematic & random errors was applied to analyze the accuracy of the test data. With the purpose of reducing random error, five measurement values at the steady state would be collected in the interval of three minutes under the setting condition.

4 Results and discussion

The heating performances of the SCRCVI system were studied by varying the f and injection pressure P_{inj}. Based on the experimental tests, the heating capacity Q_h variations of the SCRCVI system and the CSVC system were shown in Figure 5. The results indicated that the increasing rate of the SCRCVI system heating capacity decreased as the injection pressure increased from 650 to 1100 kPa. In addition, the heating capacity at different compressor frequencies showed the same trend. This trend could be explained by the variation and importance of the system parameters. As the injection pressure increased, the increase of injection mass

Table 2 Specification of system components.

Components	Specifications
Compressor	Type: inverter driven rotary compressor; displacement volume: 10.8 cm³ rev^{-1}; the circle radius of cylinder: 21.5 mm; the rotor radius: 17.05 mm; the length of the cylinder: 20 mm; the diameter of injection hole: 4 mm
Condenser (indoor heat exchanger)	Type: fin/tube heat exchanger (aluminum/copper), *L*-shaped; tube outer diameter: Ø6.14×0.57 mm; fin thickness: 0.1 mm; fin spacing: 1.2 mm; number of rows: 2; number of tubes: 34; dimension:700 mm×360 mm×26 mm
Evaporator (outdoor heat exchanger)	Type: fin/tube heat exchanger (aluminum/copper), *L*-shaped; tube outer diameter: Ø9.52×0.7 mm; fin thickness: 0.1 mm; fin spacing: 1.1 mm; number of rows: 2; number of tubes: 40; dimension: 880 mm×510 mm×45 mm
Electrical expansion valve	Type: electronic expansion valve control resolution: 0–500 steps
flash tank	outer diameter: 38.32 mm; volume: 185 cm³

Table 3 Experiment conditions

Operating mode	Indoor		Outdoor	
	T_{DB} (°C)	T_{WB} (°C)	T_{DB} (°C)	T_{WB} (°C)
Heating	20	15	−10	-
Refrigerant type		R410A		
Refrigerant charge		1380 g		
Compressor frequency f		60–100 Hz		
Superheated degree of the suction vapor		3–5 K		

Table 4 Instrumentation and propagated uncertainties

No.	Instrument	Type	Range	Uncertainty	Obtaining data
1	Thermocouple	T	–200°C–350°C	±0.5°C	Measured value (refrigerant-side)
2	Pressure transducer	Ceramic membrane	0–4000 kPa	±0.2% of full scale	Measured value (refrigerant-side)
3	Pressure transducer	Ceramic membrane	0–6000 kPa	±0.2 % of full scale	Measured value (refrigerant-side)
4	Temperature sensor	platinum thermistor	–50°C–300°C	±0.15°C	Measured value (air-side)
5	Pressure difference transducer	Diaphragm	0–6 bar	±0.5% of full scale	Measured value (air-side)
6	Power meter	–	0–5 kW	±0.5% of full scale	Measured value (refrigerant-side)
7	Mass flow meter	Coriolis	0–600 kg h^{-1}	±0.35% of flow rate	Measured value (refrigerant-side)
8	Refrigerant-side capacity	–	–	±3.15%	Calculated value
9	Refrigerant-side COP_h	–	–	±3.16%	Calculated value
10	Air-side capacity	–	–	±6.61%	Calculated value

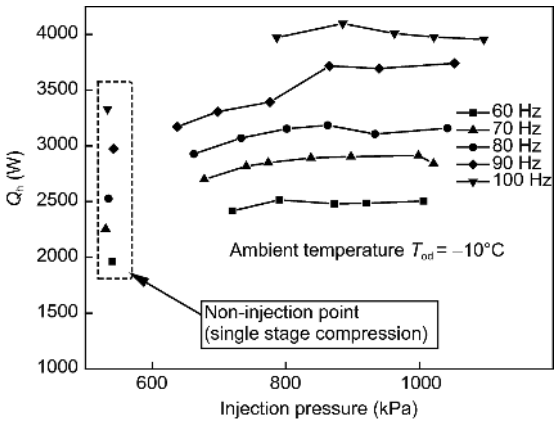

Figure 5 Variation of heating capacity with injection pressure.

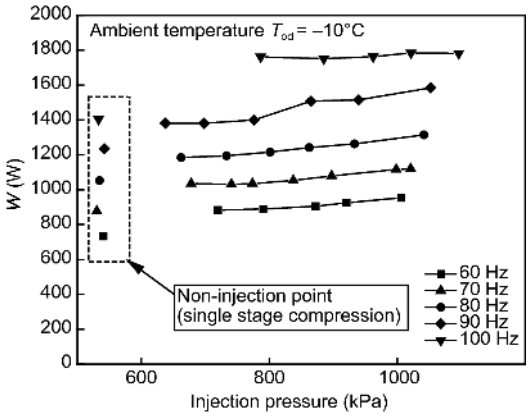

Figure 6 Variation of power consuming with injection pressure.

flow rate led to the increase of the total mass flow rate, and also enhanced the inter-cooling effect in the cylinder. Therefore, in this condition, the discharge temperature/pressure decreased, which caused the enthalpy difference of refrigerant before and after the condenser decreased slowly. However, as the injection pressure increased in the low-pressure range, the growth rate of total mass flow rate was higher than the reducing rate of enthalpy difference of refrigerant before and after the condenser, which gave great contribute to the increase of the Q_h. As the P_{inj} increased over a certain value, the Q_h of the SCRCVI system kept nearly constant due to the reduction rate of enthalpy difference of refrigerant before and after the condenser was almost synchronized with the growth rate of total mass flow rate. The increasing trend of heating capacity according to the compressor frequency can be explained by the increase of total mass flow rate and rotational speed. Under the operating condition, the heating capacities of the SCRCVI system improved about 6.65%–28.2% over that of the CSVC system. The maximum Q_h of the SCRCVI system at f=100 Hz was 62.90% higher than the maximum value at f=60 Hz. Therefore, for the cold regions, using inverter technology to drive the compressor with refrigerant injection was an effective way to improve the heating capacity.

Figure 6 shows the variation of power consuming with injection pressure. From experimental results, it could be observed that the power consuming W of the SCRCVI system was higher than that of the CSVC system. In addition, the power consuming W of the SCRCVI system obviously rise and slightly increased according to the compressor frequency and injection pressure, respectively. For the compressor frequency from 60 to 100 Hz, the power consuming W of the SCRCVI system was 11.82%–30.12% higher than that of the CSVC system. The power consuming W of the SCRCVI system at f=100 Hz increased about 94.0% (856.7 W) over that at f=60 Hz. The main reasons for this tendency were that: (i) as the injection pressure increasing, the discharge temperature and pressure decreased, the total and injection mass flow rate both increased, and the specific enthalpy of suction vapor kept constant. The shaft power of the system compressor increased slightly because the increase of total mass flow rate had an important influence on the variation of the power consuming; (ii) as the compressor frequency increasing, the rotational speed rise. Under the same injection pressure and suction pressure, the displacement volume was significantly improved with the rise of rotational speed, which finally led to the shaft power increasing obviously.

Figure 7 illustrated the variation of COP_h with injection pressure at f=60–100 Hz. As the injection pressure increasing, the COP_h of the SCRCVI system increased first and then decreased. Corresponding to the variation tendency of the COP_h, an optimum injection pressure P_{inj} could be obtained at the peaked value. In addition, the maximum COP_h of the SCRCVI system decreased as the increase of the f because the power consuming increased obviously with the f. Compared with the CSVC system, the maximum COP_h were improved about 3.73%, 7.0%, 7.91%, 2.49%, and –1.27% at the compressor frequency of 60, 70, 80, 90, and 100 Hz, respectively. Due to the increase of the SCRCVI system shaft power gave great contribute to improving the system Q_h, and the effect of refrigerant injection become weaker, the COP_h of the SCRCVI system was lower than that of the CSVC system at high compressor frequencies. Therefore, in view of the energy saving and emission reduction, the SCRCVI system should be switched to single stage compression system when the heating capacity demand could be satisfied at high compressor frequency f. Furthermore, the optimum P_{inj} corresponding to the maximum COP_h increases according to the f. From the sight glass installed on the injection pipe, it can be seen that a little liquid refrigerant was injected into the compressor as the SCRCVI system worked at the optimum injection pressure P_{inj}.

Figure 8 displays the variation of total mass flow rate with

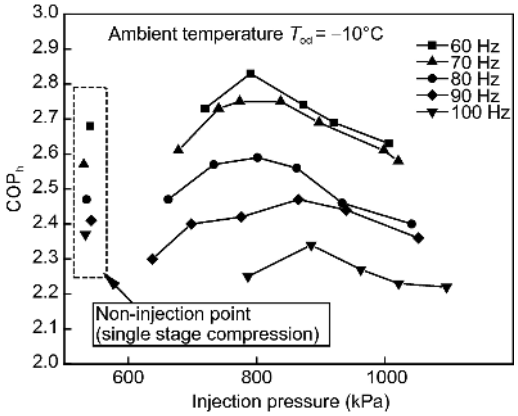

Figure 7 Variation of COP_h with injection pressure.

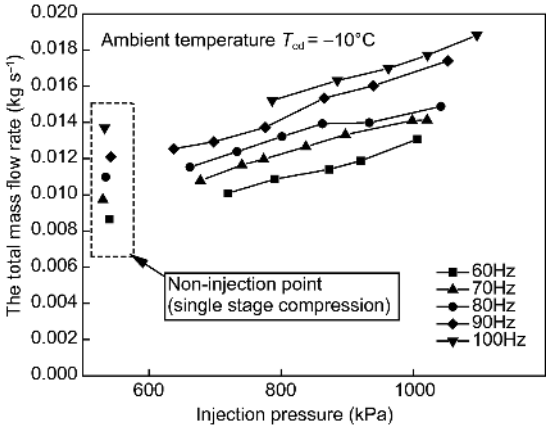

Figure 8 Variation of total mass flow rate with injection pressure.

injection pressure at the compressor frequency ranging from 60 to 100 Hz. The total mass flow rate of the SCRCVI system steadily increased with the P_{inj} and the f. Compared with the CSVC system, the average total mass flow rate of the SCRCVI system was improved about 24.68% under the given condition. For the CSVC system, the average growth rate of the total mass flow rate was about 0.1 g s^{-1} Hz^{-1}. However, the average growth rate for the SCRCVI system was 0.136 g s^{-1} Hz^{-1} and 1.056×10^{-2} g s^{-1} kPa^{-1}, relative to the compressor frequency and injection pressure, respectively. The reasons for the trend mentioned above were the increase of the injection mass flow rate and the rise of the rotational speed. As the injection pressure increased, the enlarged pressure difference between P_{inj} and P_{wc}, and the decline of specific volume at the injection pipe led to the increasing of the injection mass flow rate eventually.

The variation of discharge temperature with injection pressure at different compressor frequency is shown in Figure 9. It could be observed that the discharge temperature of the SCRCVI system declined according to the injection pressure at the same compressor frequency and increased with the compressor frequency at the same injection pressure. Compared with the CSVC system, the discharge temperature of the SCRCVI system was higher at low injection pressure and then decreased to a lower value when the injection pressure increased to high enough. As the injection pressure increased, the decrease of discharge temperature was due to the increase of injection refrigerant, which enhanced the inter-cooling effect. As the injection pressure was low, the discharge temperature of the SCRCVI system was higher because of the specific injection structure. The specific enthalpy of the injection vapor was about 423–427 kJ kg^{-1} at low injection pressure, which was slightly higher than the suction vapor specific enthalpy 420 kJ kg^{-1}. The injected vapor would heat the suction vapor at the early compression processes. So when the injection pressure was quite low, there was no enough refrigerants to cool down the vapor in the working chamber at the latter compression process.

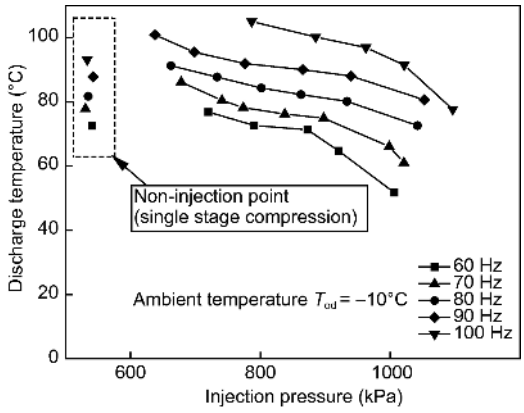

Figure 9 Variation of discharge temperature with injection pressure.

Figure 10 shows the variation of discharge pressure and suction pressure of the SCRCVI system and the CSVC system with compressor frequency at the ambient temperature T_{od}=−10°C. It should be noted that the injection pressure of the SCRCVI system was fixed at the optimum value corresponding to the optimum heating performance. The test results showed that due to the addition of the refrigerant injection process, the average increment of the SCRCVI system discharge pressure was about 7.1%, relative to that of the CSVC system. However, for the suction pressure under the same operation condition, there was no obvious difference between the SCRCVI system and the CSVC system.

The comparison between the SCRCVI system discharge temperature and the CSVC system discharge temperature under the same working condition was shown in Figure 11. As the compressor frequency increased, the increasing trend in variation of the discharge temperature for the SCRCVI system was consistent with that of the CSVC system. When the f was lower than 80 Hz, the discharge temperature difference between the two systems was smaller than 1.5°C. However, as the f continually increased, the discharge tem-

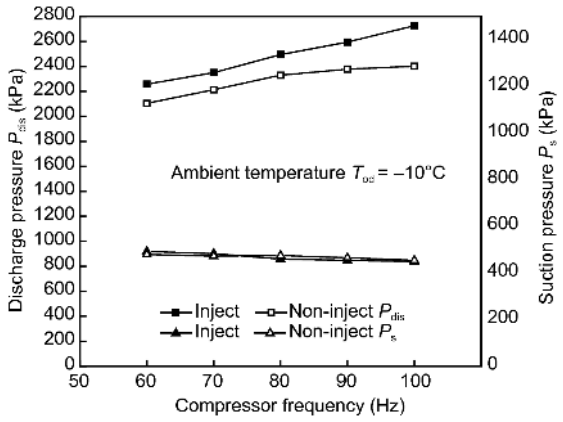

Figure 10 Variation of discharge pressure and suction pressure with compressor frequency.

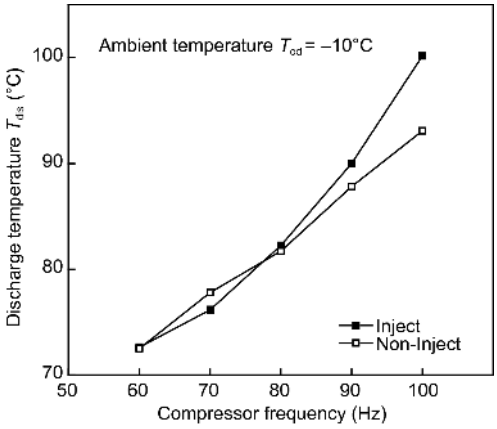

Figure 11 Variation of discharge temperature with compressor frequency.

perature difference was enlarged to 7.09°C at the compressor frequency of 100 Hz. From the comparison, it can be seen that the SCRCVI system had a higher T_{dis} at the high f, which was harmful to the efficiency of compression. When the injection pressure further increased, the T_{dis} of the SCRCVI system would be reduced to quite a low level eventually, and this also caused the SCRCVI system heating performance degraded rapidly.

Figure 12 shows the variation of R_m and R_p of the SCRCVI system according to the f at the optimum injection pressure. The variation trend of R_m was almost synchronized with that of the injection pressure ratio R_p. Both of the R_m and R_p were increased first and then decreased with the increase of the compressor frequency. For the compressor frequency from 60 to 100 Hz, the R_m and R_p were in the range of 0.192–0.217 and 0.174–0.212, respectively. This trend could be explained as follows: the injection mass flow rate was mainly determined by the injection pressure while the total mass flow rate was mainly determined by the compressor frequency. As the increase of the compressor frequency, the optimum injection pressure just increased about 85 kPa, and the suction

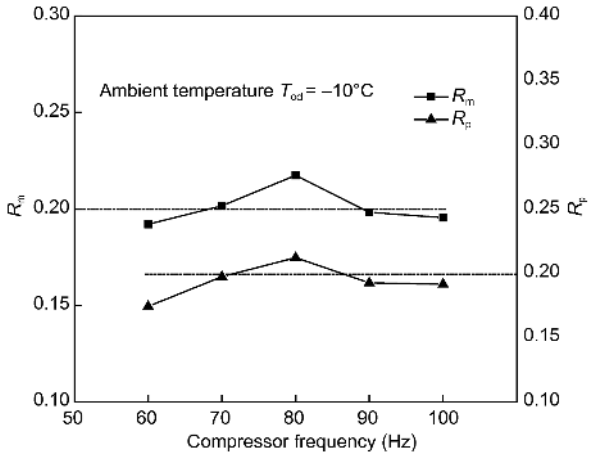

Figure 12 Variation of R_m and R_p with compressor frequency.

pressure also decreased slightly. It meant that the total mass flow rate increased rapidly while the injection mass flow rate remained to keep a lower growth rate as the compressor frequency increased under the given testing condition. Therefore, the compressor frequency should be limited to an appropriate range in order to achieve a high heating performance and safe operation if the heating capacity could meet the room heating load.

The variation of optimum injection pressure P_{inj} and (P_{inj}–P_s) according to compressor frequency were shown in Figure 13. From the experimental results, it can be seen that both the optimum injection pressure and (P_{inj}–P_s) increased with increasing compressor frequency. The changing trend of optimum injection pressure P_{inj} and (P_{inj}–P_s) could be explained by the variation of the optimum heating performance (COP_h). When the compressor frequency varied from 60 to 100 Hz at the ambient temperature T_{od}=–10°C, the optimum injection pressure P_{inj} and (P_{inj}–P_s) varied in the range of 800–886 and 308–436 kPa, respectively. The (P_{inj}–P_s) increased linearly with compressor frequency. These trends were reliably used to optimize the system design and the control strategy. Furthermore, the pressure difference between suction pressure and injection pressure (P_{inj}–P_s) could be adopted as the signal to control the opening of the upper stage electronic expansion valve EEV1 of the SCRCVI system.

5 Conclusions

The heating performances of an R410A flash tank refrigerant injection system with single cylinder rotary compressor were studied by changing the f and the P_{inj} at the ambient temperature T_{od}=–10°C. A comprehensive comparison between the SCRCVI system and CSVC system was conducted to evaluate the space for optimization. The test results indicated that the SCRCVI could enhance the heating performance effectively. The Q_h and COP_h of the SCRCVI system at the

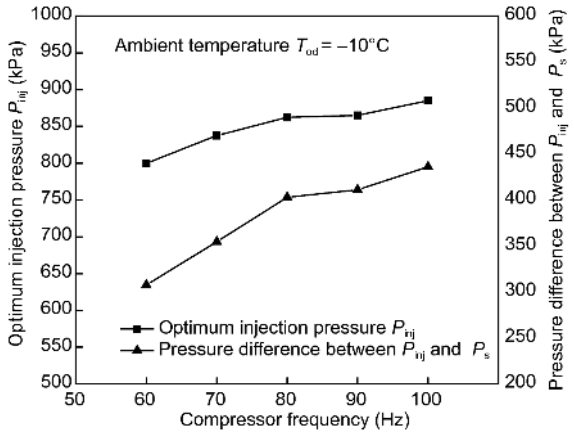

Figure 13 Variation of optimum injection pressure and (P_{inj}–P_s) with compressor frequency.

intermediate injection pressure could be improved by 28.2% and 7.91% over that of the CSVC system, respectively. The peak value of COP_h could be obtained at the optimum injection pressure. In addition, the peak COP_h of the SCRCVI system decreased as the increase of the frequency, and the maximum COP_h was even lower than that of the CSVC system at high compressor frequency. Therefore, in view of the energy saving and emission reduction, the SCRCVI system should be switched to single stage compression system when the heating capacity demand could be satisfied at high compressor frequency *f*. Compared with the CSVC system, the average total mass flow rate of the SCRCVI system was improved by 24.68% under the given condition. The discharge temperature of the SCRCVI system declined according to the injection pressure. When the SCRCVI system worked at the optimum injection pressure, the variation trends of the discharge pressure P_{dis}, suction pressure P_s, discharge temperature T_{dis}, injection mass flow ratio R_m, injection pressure ratio R_p, and (P_{inj}–P_s) according to compressor frequency were investigated. For the compressor frequency from 60 to 100 Hz, the R_m, R_p, optimum injection pressure P_{inj} and (P_{inj}–P_s) were varied in the range of 0.192–0.217, 0.174–0.212, 800–886 and 308–436 kPa, respectively. In addition, the (P_{inj}–P_s) increased linearly with compressor frequency. The parameter of (P_{inj}–P_s) could be adopted as the signals to control the R_m and the opening of the upper stage electronic expansion valve EEV1 with the purpose of obtaining the optimum heating performance.

This work was supported by the South Wisdom Valley Innovative Research Team Program (serial number: Shunde District of Foshan City Government Office [2014] No.365) and the 2017 Guangzhou Collaborative Innovation Major Projects (Grant Nos. 201604016048 and 201604016069).

1 Heo J, Jeong M W, Baek C, et al. Comparison of the heating performance of air-source heat pumps using various types of refrigerant injection. Int J Refrigeration, 2011, 34: 444–453
2 Xu X, Hwang Y, Radermacher R. Refrigerant injection for heat pumping/air conditioning systems: Literature review and challenges discussions. Int J Refrigeration, 2011, 34: 402–415
3 Xu S X, Ma G Y. Air-source heat pump coupled with economized vapor injection scroll compressor and ejector: Design and experimental research. Sci China Tech Sci, 2010, 53: 782–788
4 Banister C J, Collins M R. Development and performance of a dual tank solar-assisted heat pump system. Appl Energy, 2015, 149: 125–132
5 Lv X, Yan G, Yu J. Solar-assisted auto-cascade heat pump cycle with zeotropic mixture R32/R290 for small water heaters. Renew Energy, 2015, 76: 167–172
6 Boahen S, Choi J M. Research trend of cascade heat pumps. Sci China Tech Sci, 2017, 60: 1597–1615
7 Lazzarin R, Noro M. Experimental comparison of electronic and thermostatic expansion valves performances in an air conditioning plant. Int J Refrigeration, 2008, 31: 113–118
8 Chen Z S, Tao W Q, Zhu Y W, et al. Performance analysis of air-water dual source heat pump water heater with heat recovery. Sci China Tech Sci, 2012, 55: 2148–2156
9 Song J, Lee K, Jeong Y, et al. Heating performance of a ground source heat pump system installed in a school building. Sci China Tech Sci, 2010, 53: 80–84
10 Adhikari R S, Aste N, Manfren M, et al. Energy savings through variable speed compressor heat pump systems. Energy Procedia, 2012, 14: 1337–1342
11 Qiao H, Aute V, Radermacher R. Transient modeling of a flash tank vapor injection heat pump system–Part I: Model development. Int J Refrigeration, 2015, 49: 169–182
12 Qiao H, Xu X, Aute V, et al. Transient modeling of a flash tank vapor injection heat pump system–Part II: Simulation results and experimental validation. Int J Refrigeration, 2015, 49: 183–194
13 Qiao H, Aute V, Radermacher R. Dynamic modeling and characteristic analysis of a two-stage vapor injection heat pump system under frosting conditions. Int J Refrigeration, 2017, 84: 181–197
14 Redón A, Navarro-Peris E, Pitarch M, et al. Analysis and optimization of subcritical two-stage vapor injection heat pump systems. Appl Energy, 2014, 124: 231–240
15 Wang B, Shi W, Han L, et al. Optimization of refrigeration system with gas-injected scroll compressor. Int J Refrigeration, 2009, 32: 1544–1554
16 Wang B, Li X, Shi W. A general geometrical model of scroll compressors based on discretional initial angles of involute. Int J Refrigeration, 2005, 28: 958–966
17 Wang B, Shi W, Li X, et al. Numerical research on the scroll compressor with refrigeration injection. Appl Thermal Eng, 2008, 28: 440–449
18 Wang B, Shi W, Li X. Numerical analysis on the effects of refrigerant injection on the scroll compressor. Appl Thermal Eng, 2009, 29: 37–46
19 Park Y C, Kim Y, Cho H. Thermodynamic analysis on the performance of a variable speed scroll compressor with refrigerant injection. Int J Refrigeration, 2002, 25: 1072–1082
20 Cho I Y, Bin Ko S, Kim Y. Optimization of injection holes in symmetric and asymmetric scroll compressors with vapor injection. Int J Refrigeration, 2012, 35: 850–860
21 Dardenne L, Fraccari E, Maggioni A, et al. Semi-empirical modelling of a variable speed scroll compressor with vapour injection. Int J Refrigeration, 2015, 54: 76–87
22 Heo J, Jeong M W, Kim Y. Effects of flash tank vapor injection on the heating performance of an inverter-driven heat pump for cold regions. Int J Refrigeration, 2010, 33: 848–855
23 Wang X, Hwang Y, Radermacher R. Two-stage heat pump system with vapor-injected scroll compressor using R410A as a refrigerant. Int J Refrigeration, 2009, 32: 1442–1451
24 Ma G Y, Zhao H X. Experimental study of a heat pump system with flash-tank coupled with scroll compressor. Energy Buildings, 2008, 40: 697–701

25 Xu X, Hwang Y, Radermacher R. Transient and steady-state experimental investigation of flash tank vapor injection heat pump cycle control strategy. Int J Refrigeration, 2011, 34: 1922–1933
26 Xu X, Hwang Y, Radermacher R. Performance comparison of R410A and R32 in vapor injection cycles. Int J Refrigeration, 2013, 36: 892–903
27 Baek C, Lee E, Kang H, et al. Experimental Study on the heating performance of a CO_2 heat pump with gas injection. In: Proceedings of International Refrigeration and Air Conditioning Conference. West Lafayette: Purdue University, 2008
28 Baek C, Heo J, Jung J, et al. Effects of vapor injection techniques on the heating performance of a CO_2 heat pump at low ambient temperatures. Int J Refrigeration, 2014, 43: 26–35
29 Jia Q, Feng L, Yan G. Experimental research on heating performance of rotary compression system with vapor injection (in Chinese). J Refrigeration, 2015, 36: 65–70
30 Jia Q, Feng L, Yan G. Experimental research on rotary compression system with vapor injection (in Chinese). Refrigeration Air-Cond, 2014, 14: 128–141
31 Wang B, Liu X, Shi W. Comparative research on air conditioner with gas-injected rotary compressor through injection port on blade. Appl Thermal Eng, 2016, 106: 67–75
32 Liu X, Wang B, Shi W, et al. A novel vapor injection structure on the blade of a rotary compressor. Appl Thermal Eng, 2016, 100: 1219–1228
33 Wang B, Liu X, Shi W. Performance improvement of air source heat pump using gas-injected rotary compressor through port on blade. Int J Refrigeration, 2017, 73: 91–98